Journal of Advanced Research 25 (2020) 235–242

Contents lists available at ScienceDirect

Journal of Advanced Research

journal homepage: www.elsevier.com/locate/jare

# Frequency bifurcation in a series-series compensated fractional-order inductive power transfer system

Xujian Shu, Bo Zhang *, Chao Rong, Yanwei Jiang

*School of Electric Power Engineering, South China University of Technology, Street Wushan, 510641, China*

## GRAPHICAL ABSTRACT

The frequency bifurcation in the fractional-order inductive power transfer system with series-series compensation topology is analyzed, in which the working range and transfer characteristics of the conventional inductive power transfer system can be improved by adjusting the fractional order.

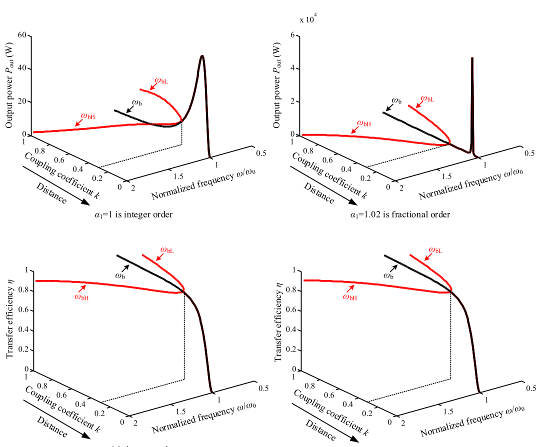


## ARTICLE INFO

*Article history:*
Received 11 February 2020
Revised 6 April 2020
Accepted 21 April 2020
Available online 24 April 2020

*Keywords:*
Frequency bifurcation
Fractional order
Inductive power transfer
Series-series compensated

## ABSTRACT

This paper reveals and analyzes the frequency bifurcation phenomena in the fractional-order inductive power transfer (FOIPT) system with series-series compensation topology. Using fractional calculus theory and electric circuit theory, the circuit model of the series-series compensated FOIPT system is first proposed, then taking the case of a single variable fractional order as an example, three frequency analytical solutions of frequency bifurcation equation are solved by using Taylor expansion method. By analyzing the three bifurcation frequencies solved, it can be found that the frequency bifurcation phenomenon can be effectively eliminated by controlling the fractional order, and the boundary of critical distance and critical load is reduced, thereby expanding the working range of the conventional inductive power transfer (IPT) system. Furthermore, the output power and transfer efficiency at the three bifurcation frequencies are analyzed, it can be observed that the output power and transfer efficiency at the high bifurcation frequency and low bifurcation frequency are close and basically keep constant against the variation of transfer distance, and the output power is obviously higher than that at the intrinsic frequency. In addition, the output power at the three bifurcation frequencies can be significantly improved

Peer review under responsibility of Cairo University.
* Corresponding author.
*E-mail address:* epbzhang@scut.edu.cn (B. Zhang).

https://doi.org/10.1016/j.jare.2020.04.010
2090-1232/

by adjusting the fractional order. Finally, the experimental prototype of FOIPT is built, and the experimental results verify the validity of theoretical analysis.


## Introduction

Fractional calculus was born as early as 300 years ago, dating back to the Leibniz's note in his letter to L'Hospital [1]. For three centuries, the theory of fractional calculus developed mainly as a pure mathematical theory. However, during the last five decades, fractional calculus is present in the field of electrical engineering, including circuit theory [2], chaotic system [3] and control system [4], etc. In the fractional-order (FO) circuit analysis, the impedance properties of FO $RL_{\beta}$ and $RC_{\alpha}$ circuit were studied in [5,6], the step and square wave responses of the FO $RC_{\alpha}$ circuit were studied in [7], resonance phenomena of FO $RL_{\beta}C_{\alpha}$ circuit was analyzed in [8] where the quality factor and resonance frequency of the circuit can be adjusted freely, and a generalized method of solving transient states of $RL_{\beta}C_{\alpha}$ circuit was described in [9]. In the FO components, the generalized concept of fractional-order mutual inductance (FOMI) was proposed in [10], in which a special case that the orders of primary and secondary side are equal are analyzed and the equivalent T-model of FOMI was presented. In addition, the construction and implementation of FO inductors and capacitors are investigated in [11–16], the finite element approximation method of using $RL$ or $RC$ ladder structures to approximating the impedances of FO elements is the most common [11], but the fractional order is less than 1 and the different fractional orders require to change all the parameters of circuit. The research on the construction of fractional-order capacitors (FOC) is especially abundant, including the realization of FOC based on electrochemistry theory [12], standard silicon process [13], the combination operational amplifiers and passive elements [14,15], and power electronic converter [16], in which the most valuable for engineering applications is the use of power electronic converter to realize the high power FOC with order greater than 1.

Moreover, wireless power transfer (WPT) technology has attracted more attention both in academia and industry in recent years. However, the modeling and characteristic analysis of the conventional WPT system are based on integer-order inductance and capacitance elements, its inherent problems, such as medium distance but high resonant frequency and low output power, etc., have prevented the WPT technology from being fully commercialized and civilianized, thus, it is great significance to explore the novel WPT. In fact, the ideal integer-order inductors and capacitors do not exist [17,18], the orders of most inductors and capacitors in the practical application are close to 1, so their fractional-order characteristics are neglected. Inspired by the above statement, the fractional-order wireless power transfer (FOWPT) have emerged [19]. The circuit model was established in [20], and the output power, transfer efficiency and resonant frequency were analyzed, it is proved that FOWPT system has better transfer performance and greater design freedom. Meanwhile, the fractional coupled model of FOWPT system was presented based on coupled-mode theory [21], which provides a valuable tool for the analysis of FOWPT system, constant current output that is independent of load was achieved [22] and a FOWPT insensitive to resonant frequency was proposed [23]. However, there is no literature on the study of reactive compensation, frequency bifurcation and transfer characteristics of FOIPT system.

Frequency bifurcation occurs under certain conditions, such as misalignment (coupling coefficient changes), load changes, etc., which is one of the most important characteristics of the traditional IPT system and adversely affects the efficient and stable operation of the system [24]. In the FOIPT system composed of fractional-order elements, there may be more unique and novel properties and associated dynamics. Therefore, to better understand the merit of the FOIPT system, it is extremely important to study the frequency bifurcation and transfer characteristics of the FOIPT system to achieve an efficient power transfer.

In this paper, the frequency bifurcation phenomenon and transfer characteristics of FOIPT system were first proposed and analyzed, which provides a preliminary theoretical basis for the further development and application of FOIPT system. In Section 'System structure and circuit model', based on fractional calculus and circuit theory, the circuit model of FOIPT system was established, and the general expressions of output power and transfer efficiency were given. In Section 'Frequency bifurcation and transfer characteristics', the bifurcation frequency analytical solutions are first solved by Taylor expansion, which is beneficial to visually distinguish the three bifurcation frequencies and determine the bifurcation conditions. Then, the frequency bifurcation properties and transfer characteristics are analyzed in detail, which provides a theoretical basis for the good understanding and design of FOIPT system. Section 'Experimental verification' gives the results of experimental verification and Section 'Conclusions' elaborates the conclusions.

## System structure and circuit model

In order to study the frequency bifurcation phenomena of the FOIPT system, we consider a series-series compensated configuration, the equivalent circuit diagram is shown in Fig. 1. In general, a series-series compensated FOIPT consists of an ac power source $u_s$, primary-side circuit, secondary-side circuit and load $R_L$. $M_{\gamma}$ is FOMI with order $\gamma\in(0,2)$, which is used to transfer energy between primary side and secondary side. The primary-side circuit is composed of a fractional-order inductance (FOI) $L_{\beta1}$ with order $\beta_1\in(0,2)$, a fractional-order compensated capacitance (FOCC) $C_{\alpha1}$ with order $\alpha_1\in(0,2)$ and an internal resistance $R_1$. The secondary-side circuit is comprised of a FOI $L_{\beta2}$ with order $\beta_2\in(0,2)$, a FOCC $C_{\alpha2}$ with order $\alpha_2\in(0,2)$ and an internal resistance $R_2$.

Based on Kirchhoff's voltage and current laws, the differential equations of the FOIPT system can be written as

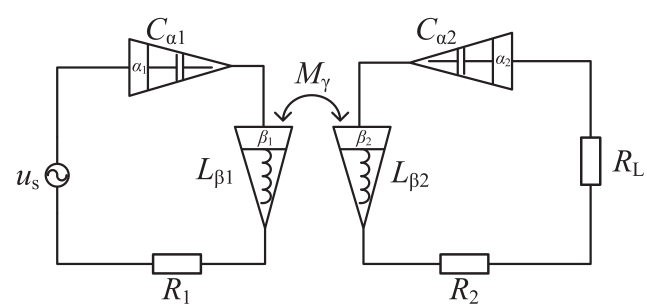


**Fig. 1.** The equivalent circuit diagram of a series-series compensated FOIPT system.

$$\begin{cases} u_s = u_{C1} + L_{\beta 1}\frac{d^{\beta_1} i_{L1}}{dt^{\beta_1}} + M_\gamma \frac{d^{\gamma} i_{L2}}{dt^{\gamma}} + R_1 i_{L1} \\ i_{L1} = C_{\alpha 1}\frac{d^{\alpha_1} u_{C1}}{dt^{\alpha_1}} \\ 0 = u_{C2} + L_{\beta 2}\frac{d^{\beta_2} i_{L2}}{dt^{\beta_2}} + M_\gamma \frac{d^{\gamma} i_{L1}}{dt^{\gamma}} + (R_2 + R_L) i_{L2} \\ i_{L2} = C_{\alpha 2}\frac{d^{\alpha_2} u_{C2}}{dt^{\alpha_2}} \end{cases} \quad (1)$$

Assuming zero initial conditions and applying the Laplace transform to (1), we have

$$\begin{cases} U_s(s) = U_{C1}(s) + (s^{\beta_1} L_{\beta 1} + R_1) I_{L1}(s) + s^{\gamma} M_\gamma I_{L2}(s) \\ I_{L1}(s) = s^{\alpha_1} C_{\alpha 1} U_{C1}(s) \\ 0 = U_{C2}(s) + \left[s^{\beta_2} L_{\beta 2} + (R_2 + R_L)\right] I_{L2}(s) + s^{\gamma} M_\gamma I_{L1}(s) \\ I_{L2}(s) = s^{\alpha_2} C_{\alpha 2} U_{C2}(s) \end{cases} \quad (2)$$

where $s$ is Laplace transform operator.

Knowing that $s = j\omega$, the impedance of FOIs can be described as

$$\begin{aligned} Z_{L\beta n} &= (j\omega)^{\beta_n} L_{\beta n} = R_{L\beta n\_eq} + j\omega L_{L\beta n\_eq} \\ &= \omega^{\beta_n} L_{\beta n}\cos\left(\tfrac{\beta_n \pi}{2}\right) + j\omega\left[\omega^{\beta_n - 1} L_{\beta n}\sin\left(\tfrac{\beta_n \pi}{2}\right)\right] \end{aligned} \quad (3)$$

The impedance of FOCCs can be given as

$$\begin{aligned} Z_{C\alpha n} &= \frac{1}{(j\omega)^{\alpha_n} C_{\alpha n}} = R_{C\alpha n\_eq} - j\frac{1}{\omega C_{C\alpha n\_eq}} \\ &= \frac{1}{\omega^{\alpha_n} C_{\alpha n}}\cos\left(\frac{\alpha_n \pi}{2}\right) - j\frac{1}{\omega \frac{\omega^{\alpha_n - 1} C_{\alpha n}}{\sin\left(\frac{\alpha_n \pi}{2}\right)}} \end{aligned} \quad (4)$$

The impedance of FOMI can be written as

$$\begin{aligned} Z_{M\gamma} &= (j\omega)^{\gamma} M_\gamma = R_{M\_eq} + j\omega M_{\gamma\_eq} \\ &= \omega^{\gamma} M_\gamma \cos\left(\frac{\gamma\pi}{2}\right) + j\omega\left[\omega^{\gamma - 1} M_\gamma \sin\left(\frac{\gamma\pi}{2}\right)\right] \end{aligned} \quad (5)$$

where the subscript n = 1, 2 represents the primary side and secondary side, respectively. $R_{L\beta n\_eq}$ and $L_{L\beta n\_eq}$ are equivalent integer-order frequency-dependent resistance and inductance of the FOI, $R_{C\alpha n\_eq}$ and $C_{C\alpha n\_eq}$ are equivalent integer-order frequency-dependent resistance and capacitance of the FOCC. $R_{M\_eq}$ and $M_{\gamma\_eq}$ are equivalent integer-order frequency-dependent resistance and mutual inductance of the FOMI.

And the input impedance seen by the power source can be derived as

$$Z_{in} = R_1 + Z_{L\beta 1} + Z_{C\alpha 1} + \frac{Z_{M\gamma}^2}{R_2 + R_L + Z_{L\beta 2} + Z_{C\alpha 2}} \quad (6)$$

In addition, the currents of primary and secondary circuits can be obtained as

$$\dot{I}_{L1} = \frac{(R_2 + R_L + Z_{L\beta 2} + Z_{C\alpha 2})\dot{U}_s}{(R_1 + Z_{L\beta 1} + Z_{C\alpha 1})(R_2 + R_L + Z_{L\beta 2} + Z_{C\alpha 2}) + Z_{M\gamma}^2} \quad (7)$$

$$\dot{I}_{L2} = \frac{-Z_{M\gamma}\dot{U}_s}{(R_1 + Z_{L\beta 1} + Z_{C\alpha 1})(R_2 + R_L + Z_{L\beta 2} + Z_{C\alpha 2}) + Z_{M\gamma}^2} \quad (8)$$

And the output power and transfer efficiency of the system can be written as

$$\begin{aligned} P_{out} &= \left|\dot{I}_{L2}\right|^2 R_L \\ &= \frac{\left|Z_{M\gamma}\right|^2 U_s^2 R_L}{\left|(R_1 + Z_{L\beta 1} + Z_{C\alpha 1})(R_2 + R_L + Z_{L\beta 2} + Z_{C\alpha 2}) + Z_{M\gamma}^2\right|^2} \end{aligned} \quad (9)$$

$$\eta = \frac{R_L}{\left\{ \begin{array}{l} \left|\frac{\dot{I}_1}{\dot{I}_2}\right|^2 \left[R_1 + \mathrm{sn}(\alpha_1) R_{C\alpha 1\_eq} + \mathrm{sn}(\beta_1) R_{L\beta 1\_eq}\right] \\ + \left[R_2 + R_L + \mathrm{sn}(\alpha_2) R_{C\alpha 2\_eq} + \mathrm{sn}(\beta_2) R_{L\beta 2\_eq}\right] \end{array} \right\}} \quad (10)$$

where $U_s$ is voltage rms of power source, $\boldsymbol{sn}(x) = \begin{cases} 1, x \leqslant 1 \\ 0, x > 1 \end{cases}$ is a custom sign function that is used to indicate that the FO elements have negative resistance characteristics when the order is greater than 1, which means that their equivalent frequency-dependent resistances do not consume electric energy [16].

## Frequency bifurcation and transfer characteristics

At present, the research on FOI is still in its infancy, while the relization of the FOC with arbitury orders is relatively developed, therefore, the study of FOIPT system with various fractional orders $\alpha_n \in (0,2)$ and constant integer orders $\beta_n = \gamma = 1$ is of great significance. To simplify the analysis, in this part, only the case of various fractional order $\alpha_1$ is discussed. It is noted that the following analysis method is not only limited to the case of single fractional order $\alpha_1$, but it can be also applied to the case of multiple fractional-order parameters, including FOs of FOI and FOMI.

### *Frequency bifurcation*

Substituting $\alpha_2 = \beta_1 = \beta_2 = \gamma = 1$ and (3)–(5) into (6), the input impedance can be written as

$$\begin{aligned} Z_{in} = R_1 &+ \frac{\omega_1^{\alpha_1+1}}{\omega^{\alpha_1}} L_1 \cot\left(\tfrac{\alpha_1 \pi}{2}\right) + j\omega L_1\left(1 - \frac{\omega_1^{\alpha_1+1}}{\omega^{\alpha_1+1}}\right) \\ &+ \frac{\omega^2 M^2}{R_2 + R_L + \frac{\omega_2^{\alpha_2+1}}{\omega^{\alpha_2}} L_2 \cot\left(\frac{\alpha_2 \pi}{2}\right) + j\omega L_2\left(1 - \frac{\omega_2^{\alpha_2+1}}{\omega^{\alpha_2+1}}\right)} \end{aligned} \quad (11)$$

Here, $L_1$ and $L_2$ are inductances of the primary and secondary coils, respectively. $M$ is the mutual inductance. $\omega_1$ and $\omega_2$ are intrinsic resonant angular frequencies of primary-side $RLC_\alpha$ and secondary-side $RLC$ circuits, which are expressed as [14]

$$\omega_1 = \left[\frac{1}{L_1 C_{\alpha 1}}\sin\left(\frac{\alpha_1 \pi}{2}\right)\right]^{\frac{1}{\alpha_1+1}} \quad (12)$$

$$\omega_2 = \frac{1}{\sqrt{L_2 C_2}} \quad (13)$$

Since the frequency bifurcation phenomenon refers to the fact that the corresponding frequency has multiple values when the angle between the input AC voltage and current is equal to zero, that is, the input impedance seen by the AC power source is pure resistance, which can be described by $\mathrm{Im}(Z_{in}) = 0$. Combining with (11), we can get the bifurcation equation as

$$\begin{aligned} &\left(1 - \frac{\omega_1^{\alpha_1+1}}{\omega^{\alpha_1+1}}\right)\left[R_2 + R_L + \frac{\omega_2^{\alpha_2+1}}{\omega^{\alpha_2}} L_2 \cot\left(\tfrac{\alpha_2 \pi}{2}\right)\right]^2 + \\ &\omega^2 L_2^2 \left(1 - \frac{\omega_1^{\alpha_1+1}}{\omega^{\alpha_1+1}}\right)\left(1 - \frac{\omega_2^{\alpha_2+1}}{\omega^{\alpha_2+1}}\right)^2 - \omega^2 k^2 L_2^2 \left(1 - \frac{\omega_2^{\alpha_2+1}}{\omega^{\alpha_2+1}}\right) = 0 \end{aligned} \quad (14)$$

where $k = M/\sqrt{L_1 L_2}$ is coupled coefficient.

By carrying out the first order Taylor expansion, $(\omega_1/\omega)^{\alpha_1+1}$ and $(\omega_2/\omega)^{\alpha_2+1}$ can be approximated as

$$\frac{\omega_n^{\alpha_n+1}}{\omega^{\alpha_n+1}} \approx 1 + (\alpha_n + 1)\left(\frac{\omega_n}{\omega} - 1\right) \quad (15)$$

Assuming $\omega_1 = \omega_2 = \omega_0$ and substituting (15) into (14), we can get

$$\begin{aligned} &\left[(\alpha_1 + 1) - \tfrac{1}{2}k^2\right]\omega^3 - \omega_0\left[3(\alpha_1 + 1) - \tfrac{1}{2}k^2\right]\omega^2 \\ &+ \omega_0^2(\alpha_1 + 1)\left[\tfrac{1}{4Q_{2L}^2} + 3\right]\omega - \omega_0^3(\alpha_1 + 1)\left[\tfrac{1}{4Q_{2L}^2} + 1\right] = 0 \end{aligned} \quad (16)$$

where $Q_{2L} = Q_2 Q_L/(Q_2 + Q_L)$ is the loaded quality factor of the secondary coil, $Q_2 = \omega_0 L_2/R_2$ is the unloaded quality factor of the secondary coil, $Q_L = \omega_0 L_2 / R_L$ is external quality factor of the secondary coil.

Factoring (16), we can obtain

$$(\omega - \omega_0)\left[\omega^2 - \omega_0(2+\chi_k)\omega + \frac{\omega_0^2}{8Q_{2L}^2}\left(2+\chi_k+8Q_{2L}^2+4\chi_k Q_{2L}^2\right)\right] = 0 \tag{17}$$

where $\chi_k = k^2 / \left[(\alpha_1+1) - \frac{1}{2}k^2\right]$.

Therefore, the three angular frequency solutions of (14), which is referred as bifurcation frequencies, can be solved as

$$\omega_\text{b} = \omega_0 \tag{18}$$

$$\omega_{bH} = \omega_0\left[1 + \frac{1}{2}\chi_k + \frac{1}{2}\sqrt{(2+\chi_k)\left(\chi_k - \frac{1}{2Q_{2L}^2}\right)}\right] \tag{19}$$

$$\omega_\text{bL} = \omega_0\left[1 + \frac{1}{2}\chi_k - \frac{1}{2}\sqrt{(2+\chi_k)\left(\chi_k - \frac{1}{2Q_{2L}^2}\right)}\right] \tag{20}$$

According to the requirement that the bifurcation frequencies are nonnegative, it is possible to obtain that the above bifurcation frequencies exist if

$$k \geqslant k_{bc} = \sqrt{\frac{2(\alpha_1+1)}{1+4Q_{2L}^2}} \tag{21}$$

$$R_L \leqslant R_{Lbc} = \frac{2\omega_0 L_2 k}{\sqrt{2(\alpha_1+1) - k^2}} - R_2 \tag{22}$$

where $k_\text{bc}$, which is denoted as the bifurcation coupling coefficient, represents the value of the coupled coefficient at which frequency bifurcation occurs. $R_\text{Lbc}$ is referred as critical load, which represents the value of the load at which frequency bifurcation appears.

From (18), (19) and (20), it can be observed that $\omega_\text{b}$ depends only on intrinsic resonant angular frequency of coil, while $\omega_\text{bH}$ and $\omega_\text{bL}$ are a function of the fractional order $\alpha_1$, intrinsic resonant angular frequency $\omega_0$, coupled coefficient $k$ and loaded qualify factor $Q_\text{2L}$. By controlling $\alpha_1$, the three bifurcation frequencies can degenerate into one, the frequency bifurcation can be avoided effectively, as shown in Fig. 2, which is different from the frequency bifurcation phenomenon of the conventional integer-order IPT system. The values of parameters used in numerical simulation are $L_1$ = 42.3μH, $L_2$ = 42μH, $\omega_0$ = 2*π*50 kHz, $R_1$ = 0.25 Ω, $R_2$ = 0.27 Ω, $k$ = 0.32, $R_\text{L}$ = 3.8 Ω, $C_2$ = 241.24nF, $C_{\alpha 1}$ varies with $\alpha_1$ according to (12).

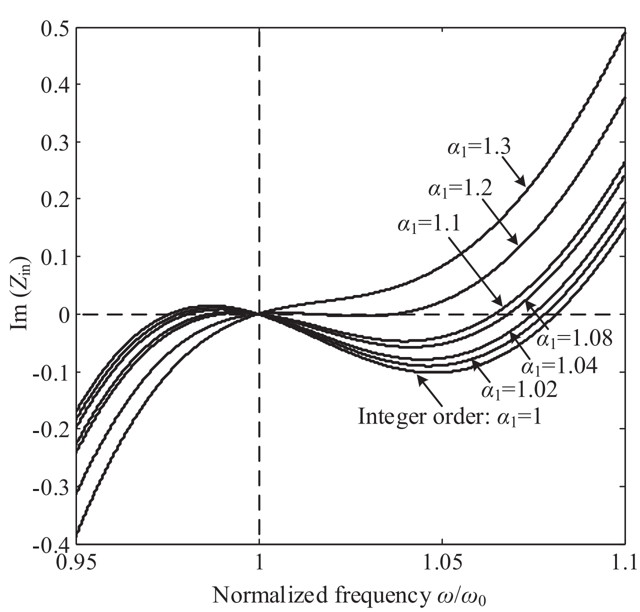


**Fig. 2.** Imaginary components of input impedance versus normalized operating frequency $\omega/\omega_0$ under $\alpha_1$ = {1, 1.02, 1.04, 1.08, 1.1, 1.2, 1.3} and $k$ = 0.32.

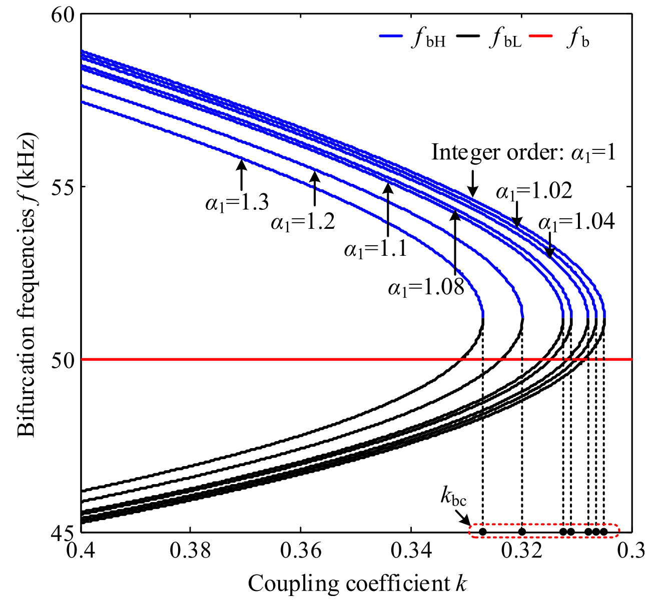


**Fig. 3.** Bifurcation frequencies versus coupling coefficient $k$ under $\alpha_1$ = {1, 1.02, 1.04, 1.08, 1.1, 1.2, 1.3} and $R_\text{L}$ = 3.8 Ω.

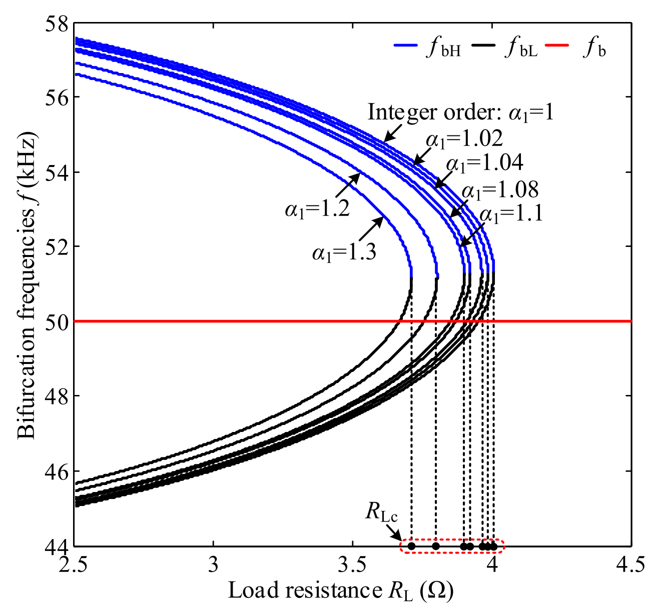


**Fig. 4.** Bifurcation frequencies versus load $R_\text{L}$ under $\alpha_1$={1, 1.02, 1.04, 1.08, 1.1, 1.2, 1.3} and $k$ = 0.32.

According to (21) and (22), it can be noted that both bifurcation coupling coefficient $k_\text{bc}$ and critical load $R_\text{Lbc}$ are determined by the loaded quality factor $Q_\text{2L}$ and fractional order $\alpha_1$, as shown in Fig. 3 and Fig. 4. With the increase of $\alpha_1$, bifurcation coupling coefficient

$k_{bc}$ increases (or, equivalently, the strong coupling region of occurrence of frequency bifurcation become narrower), which indirectly indicates that the application of FO elements can expand the distance that the IPT system effectively transfer power. Similarly, as $\alpha_1$ increases, the values of $R_{Lbc}$ gradually decreases. When the load $R_L$ is higher than this value, the frequency bifurcation disappears. In other words, the application of the FO elements can widen the range of the load compared with the integer-order IPT system. Furthermore, from Fig. 3 and Fig. 4, it can also be seen that three bifurcation frequencies degenerate into one as the coupling coefficient $k$ decreases (or as the load resistance $R_L$ increases) under a constant $\alpha_1$, once $k$ is lower than $k_{bc}$ (or $R_L$ is higher than $R_{Lbc}$), the bifurcation phenomenon disappears and the FOIPT system works at the intrinsic resonant angular frequency of coil $\omega_0$, which is similar to the bifurcation property of the traditional IPT system. Here, $f_b = \omega_b/(2\pi)$, $f_{bH} = \omega_{bH}/(2\pi)$ and $f_{bL} = \omega_{bL}/(2\pi)$. The solid blue line represents the high bifurcation frequency $f_{bH}$, the solid black line represents the low bifurcation frequency $f_{bL}$, the solid red line represents the intermediate bifurcation frequency $f_b$, which is equal to the intrinsic resonant frequency of coils $f_0 = \omega_0/(2\pi)$.

*Transfer characteristics*

Let us consider the cases of $\omega = \omega_b$, $\omega_{bH}$ or $\omega_{bL}$, substituting them into (9) and (10), the corresponding output power and transfer efficiency are presented as

$$P_{out} = \frac{\lambda_m^2 k^2 \frac{1}{\omega_0 L_1}\frac{1}{Q_L} U_s^2}{\left\{ \begin{array}{c} \left[\frac{\xi_1}{Q_{2L}^2} + \lambda_m^2 k^2 - \lambda_m^2\left(1 - \frac{1}{\lambda_m^{\alpha_1+1}}\right)\left(1 - \frac{1}{\lambda_m^2}\right)\right]^2 \\ + \lambda_m^2\left[\left(1 - \frac{1}{\lambda_m^{\alpha_1+1}}\right)\frac{1}{Q_{2L}^2} + \left(1 - \frac{1}{\lambda_m^2}\right)\xi_1\right]^2 \end{array} \right\}} \quad (23)$$

$$\eta = \frac{\frac{Q_{2L}}{Q_L}}{\frac{Q_{2L}}{k^2}\left[\frac{1}{\lambda_m^2 Q_{2L}^2} + \left(1 - \frac{1}{\lambda_m^2}\right)^2\right]\left[\frac{1}{Q_1} + \frac{\mathrm{sn}(\alpha_1)}{\lambda_m^{\alpha_1}}\cot\left(\frac{\alpha_1\pi}{2}\right)\right] + 1} \quad (24)$$

where $\xi_1 = 1/Q_1 + \cot\left(\frac{\alpha_1\pi}{2}\right)/\lambda_m^{\alpha_1}$, $Q_1 = \omega_0 L_1/R_1$ is the intrinsic quality factor of the primary coil, $\lambda_m$ (m = 1, 2 and 3) represents the normalized bifurcation frequency, which is denoted as

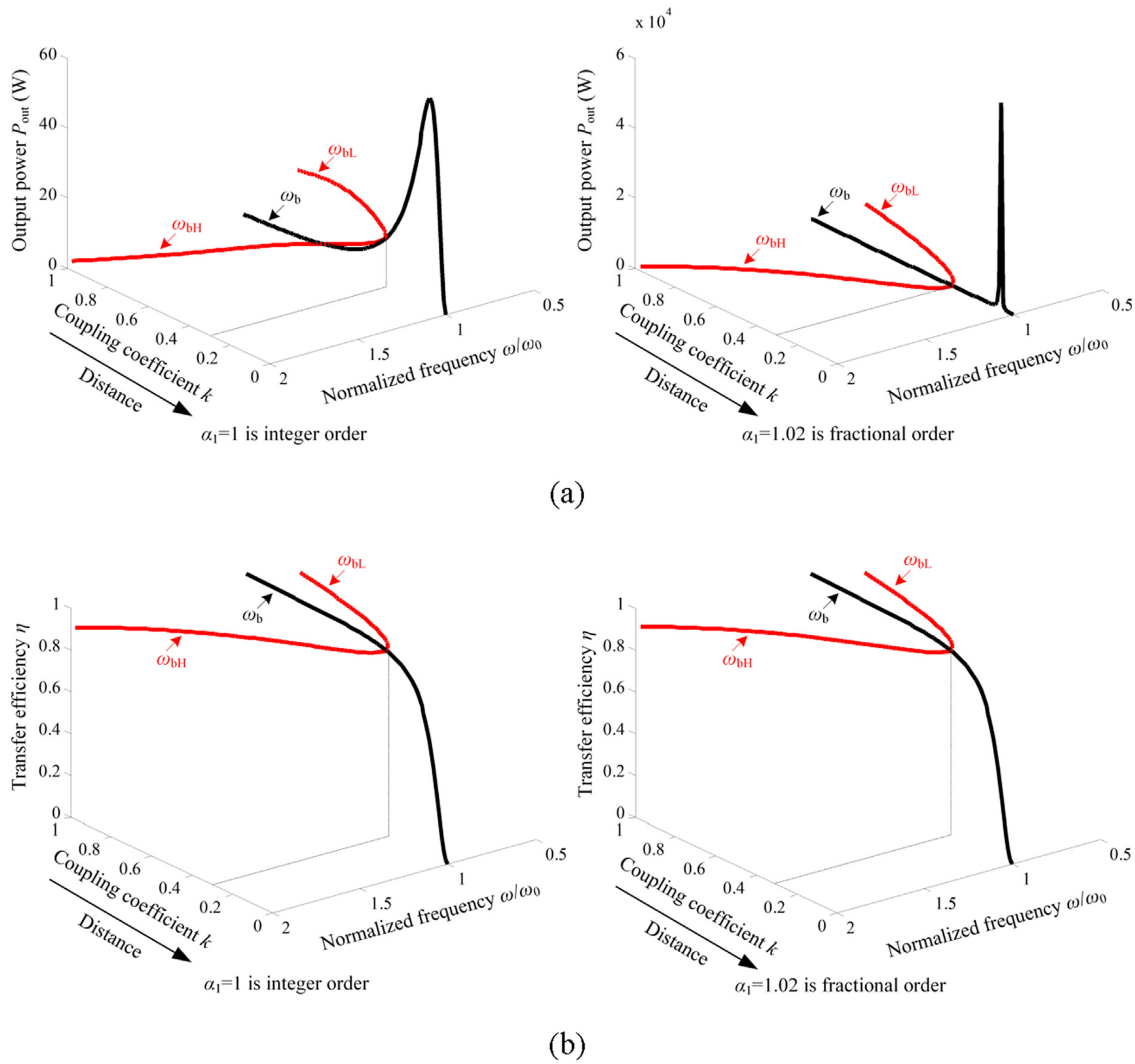


**Fig. 5.** Comparisons of output power and transfer efficiency at bifurcation frequencies between integer-order ($\alpha_1$ = 1) and fractional-order (setting $\alpha_1$ = 1.02) IPT system: (a) Output power versus coupling coefficient $k$ and normalized frequency $\omega/\omega_0$ under $\alpha_1$ = 1 and $\alpha_1$ = 1.02; (b) Transfer efficiency versus coupling coefficient $k$ and normalized frequency $\omega/\omega_0$ under $\alpha_1$ = 1 and $\alpha_1$ = 1.02.

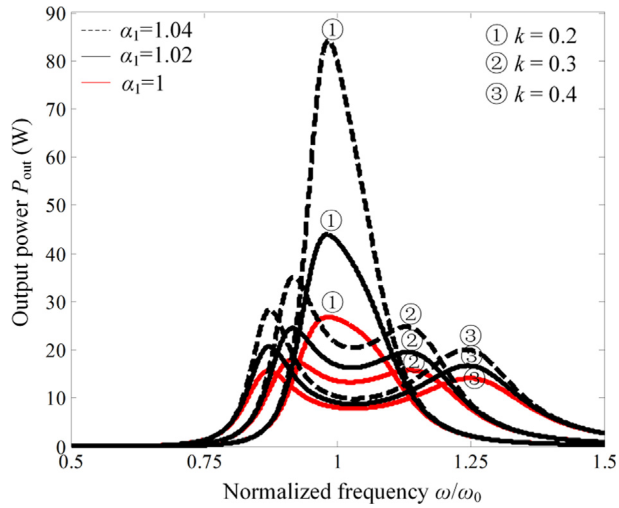


**Fig. 6.** Comparisons of the output power between the integer-order and fractional-order IPT system.

$$\begin{cases} \lambda_1 = \frac{\omega_b}{\omega_0} = 1 \\ \lambda_2 = \frac{\omega_{bH}}{\omega_0} = 1 + \frac{1}{2}\chi_k + \frac{1}{2}\sqrt{(2+\chi_k)\left(\chi_k - \frac{1}{2Q_{2L}^2}\right)} \\ \lambda_3 = \frac{\omega_{bL}}{\omega_0} = 1 + \frac{1}{2}\chi_k - \frac{1}{2}\sqrt{(2+\chi_k)\left(\chi_k - \frac{1}{2Q_{2L}^2}\right)} \end{cases} \quad (25)$$

From (23) and (24), it can be known that the output power $P_{out}$ and transfer efficiency $\eta$ of the system are the functions of the fractional order $\alpha_1$, and the output power is infinite in a certain fractional order $\alpha_0$, in which the power source is short-circuited, it is caused by the negative resistance characteristics of FOCC when $\alpha_1 > 1$, in which case the input impedance is zero, that is, the negative resistance generated by the FOCC exactly cancels out all the loss resistances of the system. Taking the case of $\lambda_m = \lambda_1 = 1$ as an example, the specific fractional order $\alpha_0$ can be derived as

$$\alpha_0 = -\frac{2}{\pi} arccot\left[\left(\frac{1}{Q_1} + k^2 Q_{2L}\right)\right] \quad (26)$$

If the fractional order $\alpha_1$ is fixed, the output power has an infinite value at a special distance, which can be derived by (26), that is

$$k_0 = \sqrt{-\frac{1}{Q_{2L}} cot\left(\frac{\pi}{2}\alpha_1\right) - \frac{1}{Q_1 Q_{2L}}} \quad (27)$$

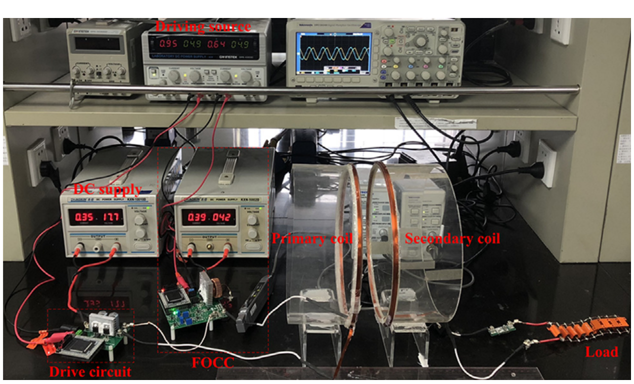


**Fig. 7.** Experimental prototype of FOIPT system.

**Table 1**
Experimental parameters.

| Parameter | Value | Parameter | Value |
|---|---|---|---|
| $V_{DC}$ | 17.7 V | $L_2$ | 42 μH |
| $L_1$ | 42.3 μH | $C_2$ | 241.24 nF |
| $\alpha_1$ | 1.02 | $R_2$ | 0.27 Ω |
| $R_1$ | 0.25 Ω | $R_L$ | 3.8 Ω |

Therefore, in the design of FOIPT system, the fractional order of FOCC should be chosen to be greater than 1 and kept away from $\alpha_0$, that is $1 < \alpha_1 < \alpha_0$. Besides, if fractional order is fixed, the system should avoid working at the above specific coupling coefficient $k_0$.

Based on the above analysis, Fig. 5 shows the comparisons of output power and transfer efficiency at bifurcation frequencies, in which the output power can be improved by controlling $\alpha_1$ to be slightly larger than 1, the output power at high bifurcation frequency $\omega_{bH}$ and low bifurcation frequency $\omega_{bH}$ are close, and so is the transfer efficiency. In order to observe the regulating effect of $\alpha_1$ on the output power more clearly, Fig. 6 shows the comparison of the output power of the integer-order and fractional-order systems with different coupling coefficients. It can be found that the introduction of FOCC can significantly improve the output power.

## Experimental verification

To practically validate the analysis of frequency bifurcation and transfer characteristics in the FOIPT system, an experimental mesurement has been setup as shown in Fig. 7, in which the FOCC is constructed by power electronic system with closed-loop control in [16]. The input voltage $U_S = \sqrt{2V_{DC}}/\pi$ comes from the output fundamental voltage of the half-bridge inverter, $V_{DC}$ is the input voltage of half-bridge inverter, and the main parameters are listed in Table 1. Here, we just give the experimental results of $\alpha_1 = 1.02$.

Fig. 8 shows the theoretical and experimental curves of three bifurcation frequencies under a certain fractional order $\alpha_1 = 1.02$, and the corresponding output power and transfer efficiency at the above three bifurcation frequencies are shown in Fig. 9. From Fig. 8, it can be found that when $\alpha_1$ is set as 1.02, the FOIPT system has three bifurcation frequencies if the coupling coefficient $k$ is

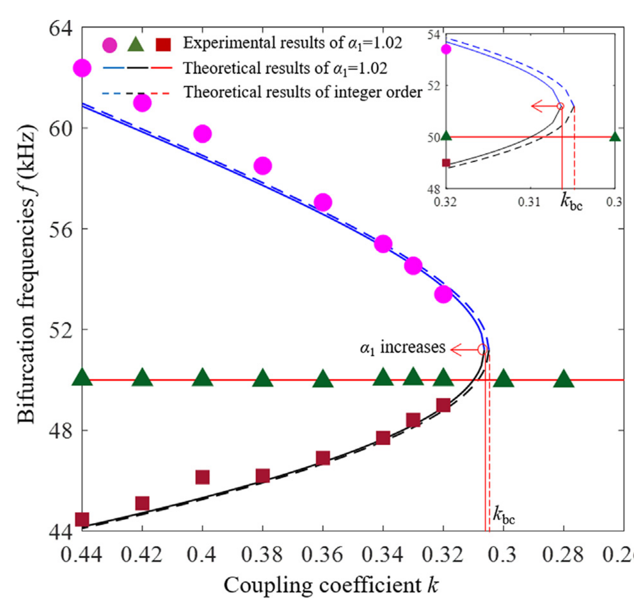


**Fig. 8.** Experimental results of bifurcation frequencies in FOIPT system under $\alpha_1$ = 1.02.

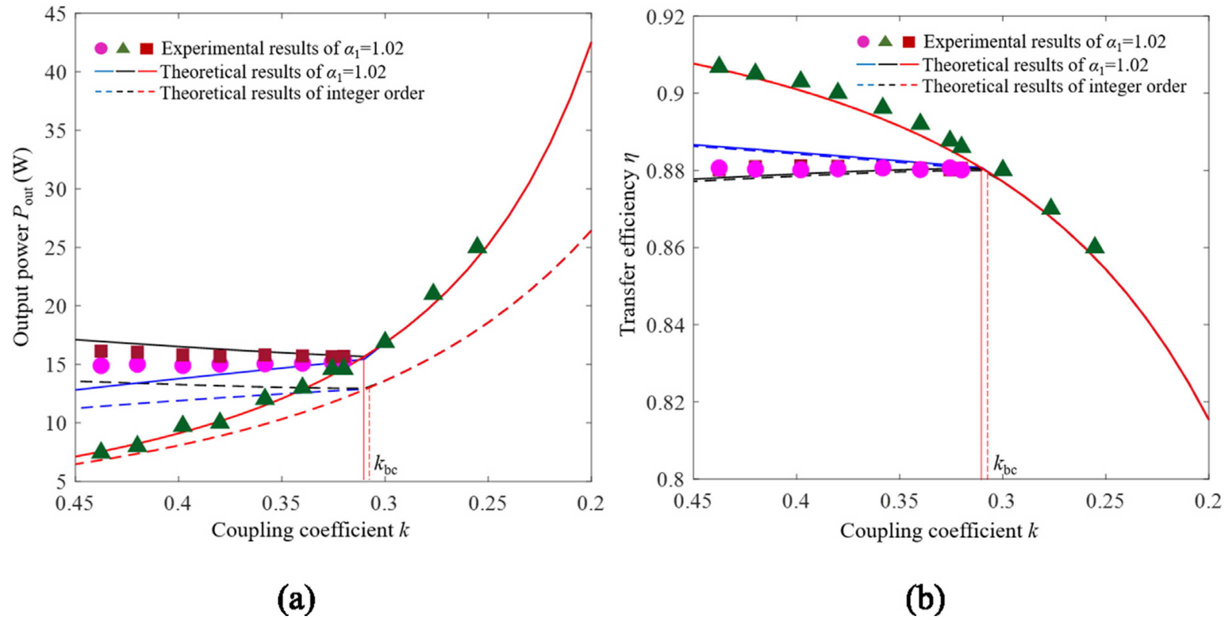


**Fig. 9.** Experimental results of output power $P_{out}$ and transfer efficiency $\eta$ in FOIPT system under $\alpha_1 = 1.02$: (a) Output power $P_{out}$ versus coupling coefficient $k$; (b) Transfer efficiency $\eta$ v versus coupling coefficient $k$.

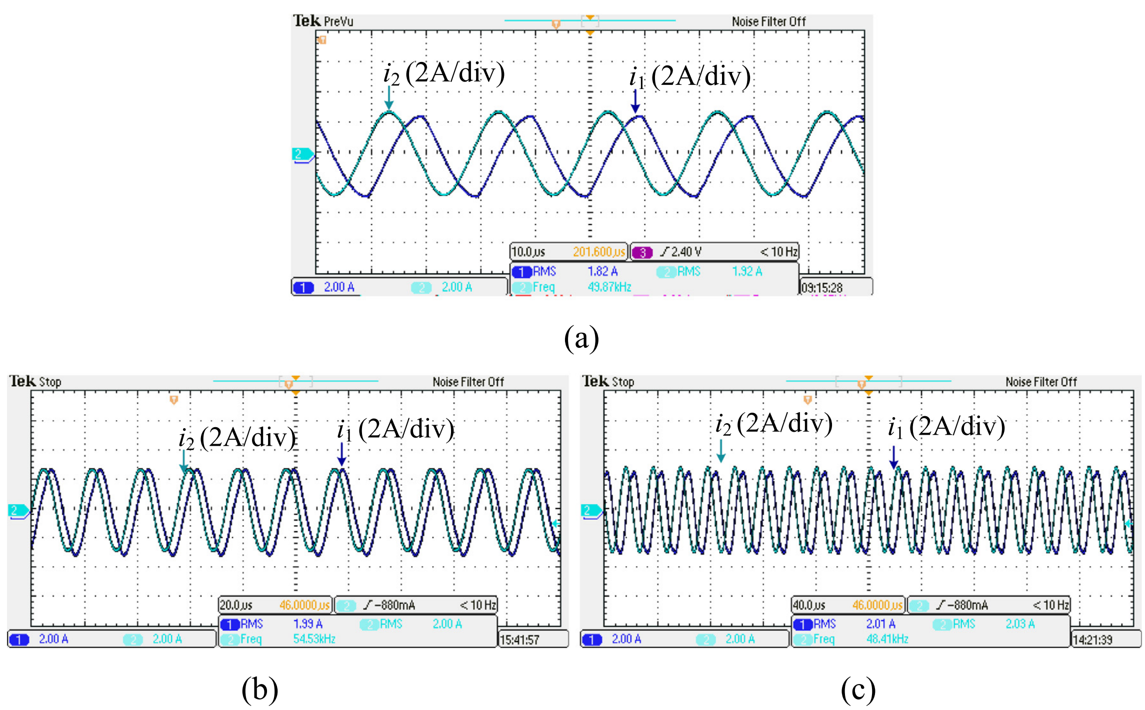


**Fig. 10.** Experimental primary-side and secondary-side current waveforms under $k = 0.32$ and $\alpha_1 = 1.02$: (a) At intrinsic resonant frequency; (b) At high bifurcation frequency; (c) At low bifurcation frequency.

greater than a certain value $k_{bc}$, which means that the frequency bifurcation occurs. Once the distance exceeds the certain value, the system works stably at the natural resonant frequency, the experimental results closely follow the theoretical curves. Comparing with the theoretical curves of integer-order IPT system, it can be seen that the critical coupling coefficient $k_{bc}$ of FOIPT system is relatively reduced, which indicates that the stable working range of the IPT system can be effectively expanded by adjusting the fractional order $\alpha_1$. Through Fig. 9, the experimental results of output power and transfer efficiency are consistent with theoretical curves, the output power and transfer efficiency of FOIPT system at high and low bifurcation frequencies are close, and less sensitive to the variation of coupling coefficient $k$. Comparing with the theoretical results of integer-order IPT system, the transfer efficiency is not affected by $\alpha_1$ when $\alpha_1$ is slightly larger than 1, while the output power is significantly improved. Fig. 10 shows the experimental waveforms of primary-side current $I_1$ and secondary-side current $I_2$ at the above bifurcation frequencies, which demonstrates the three bifurcation frequency values and the corresponding current waveforms of primary side and secondary side at a given $k = 0.32$.

## Conclusions

This paper provides the anslysis of the frequency bifurcation phenomena in the series-series compensated FOIPT system, the exact bifurcation equation is built, and the analytical solutions of bifurcation frequency, output power and transfer efficiency of the FOIPT system are derived. Theoretical analysis shows that the fractional order has a regulating effect on the frequecy bifurcation and transfer characteristic of FOIPT system, the working range of the system can be expanded, and the output power at the three bifurcation frequencies can be significantly improved. Furthermore, the theoretical analysis is confirmed by experimental results of the FOIPT system prototype. Therefore, the analysis of frequency bifurcation in this paper has an important reference value for further engineering application, such as electric vehicle (EV) charging application, portable electronic products charging application, etc., and has theoretical guiding significance for the parameter design and optimal working state of the system.

## Acknowledgements

This work was supported in part by the Key Program of the National Natural Science Foundation of China under Grant 51437005.

## Declaration of Competing Interest

The authors declare no conflict of interest.

## Compliance with Ethics Requirements

This article does not contain any studies with human or animal subjects.

## References

[1] Podlubny. Fractional differential equations. mathematics in science and engineering. San Diego: Academic Press; 1999.
[2] Radwan AG, Salama KN. Passive and active elements using fractional $L_\beta C_\alpha$ circuit. IEEE Trans Circ Syst I: Regul Pap 2011;58(10):2388–97.
[3] Doye Ibrahima N, Salama Khaled Nabil, Laleg-Kirati Taous-Meriem. Robust fractional-order proportional-integral observer for synchronization of chaotic fractional-order systems. IEEE/CAA J Automatica Sinica JAN 2019;6(1):268–77.
[4] Cajo Ricardo, Mac Thi Thoa, Plaza Douglas, Copot Cosmin, De Keyser Robain, Ionescu Clara. A survey on fractional order control techniques for unmanned aerial and ground vehicles. . IEEE Access 2019;7:66864–78.
[5] Radwan AG, Salama KN. Fractional-order *RC* and *RL* circuits. Circ Syst Signal Process 2012;31(6):1901–15.
[6] Kartci Aslihan, Agambayev Agamyrat, Herencsar Norbert, Salama Khaled N. Series-, parallel-, and inter-connection of solid-state arbitrary fractional-order capacitors: theoretical study and experimental verification. IEEE Access 2018;6:10933–43.
[7] AbdelAty AM, Radwan AG, Ahmed WA, Faied M. Charging and discharging RCα circuit under Riemann-Liouville and Caputo fractional derivatives. In: Proceeding of 13th International conference on electrical engineering/electronics, computer, telecommunications and information technology (ECTI-CON); Jun 2016.
[8] Radwan AG. Resonance and quality Factor of the $RL_\beta C_\alpha$ fractional circuit. IEEE J Emerg Sel Top Circ Syst 2013;3(3):377–85.
[9] Jakubowska Agnieszka, Walczak Janusz. Analysis of the transient state in a series circuit of the class $RL_\beta C_\alpha$. Circ Syst Signal Process 2016;35:1831–53.
[10] Soltan A, Radwan AG, Soliman AM. Fractional-order mutual inductance: Analysis and design. Int J Circ Theory Appl 2015;44(1):85–97.
[11] Sarafraz MS, Tavazoei MS. Passive realization of fractional-order impedances by a fractional element and *RLC* components: conditions and procedure. IEEE Tran Circ Syst I: Regul Pap 2016;64(3):585–95.
[12] Mondal D, Biswas K. Packaging of single-component fractional order element. IEEE Trans Device Mater Reliab 2013;13(1):73–80.
[13] Tsirimokou G, Psychalinos C, Elwakil AS, Salama KN. Experimental verification of on-chip CMOS fractional-order capacitor emulators. Electron Lett 2016;52 (15):1298–300.
[14] Semary Mourad S, Fouda Mohammed E, Hassan Hany N, Radwan Ahmed G. Realization of fractional-order capacitor based on passive symmetric network. J Adv Res 2019;18:147–59.
[15] Adhikary Avishek, Choudhary Sourabh, Sen Siddhartha. Optimal design for realizing a grounded fractional order inductor using GIC. IEEE Trans Circ Syst I: Regul Pap 2018;65(8):2411–21.
[16] Jiang Y, Zhang B. High-power fractional-order capacitor with $1<\alpha<2$ based on power converter. IEEE Trans Ind Electron 2018;65(4):3157–64.
[17] Machado JA, Galhano A. Fractional order inductive phenomena based on the skin effect. Nonlinear Dyn 2011;68(1–2):107–15.
[18] Samavati H, Hajimiri A, Shahani AR, Nasserbakht GN, Lee TH. Fractal capacitors. IEEE J Solid State Circ 1998;33(12):2035–41.
[19] Zhang B, Huang R, Qiu D. Fractional order series resonance system for wireless electric energy transmission. U.S. Patent No. 9,620,965. 11 Apr. 2017.
[20] Shu X, Zhang B. The effect of fractional orders on the transmission power and efficiency of fractional-order wireless power transmission system. Energies 2018;11(7):1774.
[21] Rong Chao, Zhang Bo, Jiang Yanwei. Analysis of a fractional-order wireless power transfer system. IEEE Trans Circ Syst II: Exp Briefs; 2019; early access.
[22] Jiang Yanwei, Zhang Bo, Zhou Jiali. A fractional-order resonant wireless power transfer system with inherently constant current output. IEEE Access 2020;8:23317–23.
[23] Jiang Yanwei, Zhang Bo. A fractional-order wireless power transfer system insensitive to resonant frequency. IEEE Trans Power Electron 2020;35 (5):5496–505.
[24] Aditya Kunwar, Williamson Sheldon S. Design guidelines to avoid bifurcation in a series-series compensated inductive power transfer system. IEEE Trans Ind Electron 2019;66(5):3973–82.